PHYSICAL REVIEW C VOLUME 15, NUMBER 2 FEBRUARY 1977

Elastic scattering of ^{40}Ca by ^{40}Ca

H. Doubre, J. C. Jacmart, E. Plagnol,* N. Poffé, M. Riou, and J. C. Roynette
Institut de Physique Nucléaire, BP No. 1, 91406 Orsay, France
(Received 19 July 1976)

Angular distributions for the elastic scattering of ^{40}Ca by ^{40}Ca at $E_{c.m.} = 64.8$, 71.8, 88, 93, 112.5, and 120 MeV and excitation functions at 60°, 70°, and 90° (c.m.) over the c.m. energy range 55–120 MeV have been measured. Strong-absorption-model and optical-model analyses are presented. The predictions of several theoretical interaction potentials are compared with the data. The absence of structure in the excitation functions is studied and explained by the large mass and charge of the colliding nuclei.

[NUCLEAR REACTIONS ^{40}Ca(^{40}Ca, ^{40}Ca), $55 \leq E_{c.m.} \leq 120$ MeV; measured $\sigma(\theta, E)$; parametrized S-matrix and optical-model analyses; semiquantal interpretation of excitation functions.]

I. INTRODUCTION

With the observation of a new strongly damped reaction mechanism between heavy ions, it has become crucial to have good estimates of the total reaction cross sections. These are usually obtained from elastic scattering data, since optical-model transmission coefficients give rather unambiguous predictions. Thus, elastic scattering measurements have found a new motivation, since a knowledge of the distribution of the incident flux between the reaction channels is of fundamental importance in heavy-ion studies. Data have been recently published[1] on elastic scattering of very heavy projectiles from heavy targets. These measurements also give primary information on the interaction potential between the nuclei at large distances.

In a program to study the interaction between ^{40}Ca nuclei, data have been collected on the elastic scattering of ^{40}Ca by ^{40}Ca. The theoretical analysis of a systematic experimental investigation of the channels fed by this system might be simplified by the closed-shell nature of this nucleus and the symmetry of the entrance channel. Recent papers have proposed a microscopic description of the dynamics of collisions between identical nuclei.[2] In our case, static and dynamic deformation effects are expected to play a less important role than with any other nucleus, and the large angular momenta involved in the scattering allow for recently developed semiclassical treatments. The ^{40}Ca + ^{40}Ca system is also a challenging test for the calculation of interaction potentials. Moreover, evidence[3] for deep-inelastic transfers at high incident energy in the ^{40}Ca + ^{40}Ca system has been presented and it would be interesting to observe the coupling of these channels to the elastic one. Finally, the experimental difficulties in heavy-ion elastic scattering are somewhat alleviated by the high (>3 MeV) energy of excited states in ^{40}Ca. This nucleus is the heaviest one for which such a situation occurs.

Aside from several angular distributions, excitation functions of the ^{40}Ca + ^{40}Ca elastic scattering are also presented. Such measurements were prompted by the observation[4] of a dramatic structure in the ^{16}O + ^{16}O elastic scattering excitation functions. The analysis[5] which was given of these data and the criteria[6] proposed for the observation of any structure in heavy-ion elastic scattering indicate that the ^{40}Ca + ^{40}Ca system could offer some analogies with the ^{16}O + ^{16}O one: (i) The identity of the incident particles reduces the number of involved partial waves which contribute at a given energy, and (ii) due to the negative Q values of all reaction channels, only the elastic one is able to carry away the initial angular momentum. From these facts, a structure can be expected in the elastic scattering excitation functions. This would be an evidence for a transparent potential where individual grazing partial waves manifest themselves. Up to now, such a transparency was only reported for nuclei close to ^{16}O. For a heavier system, as ^{28}Si + ^{28}Si, no structure was observed.[7] As far as the criteria reported above might be applied to the ^{40}Ca + ^{40}Ca system, this could be the heaviest one where a "quasi-molecular" behavior or, at least, any transparency in the interaction potential could be observed. The present study of the ^{40}Ca + ^{40}Ca elastic scattering extends from 55 to 120 MeV(c.m.); this could be a sufficient range to observe any peculiar behavior as a function of energy. In Sec. VI some implications of the nonobservation of any structure in ^{40}Ca + ^{40}Ca are considered.

Transfer data have also been collected on the same energy range and are to be published.

II. EXPERIMENTAL PROCEDURE

With heavy ions, the requirement of an unambiguous identification of elastic events leads to experimental difficulties. Two of them seem quite crucial when the masses of the colliding nuclei are large. Depending on the incident energy and on specific Q values, the discrimination between elastic scattering and few-nucleon transfer products can become very critical. Furthermore, inelastic scattering strongly excites low-lying states and, at large angles, can be much more likely than elastic scattering. As already mentioned, the $^{40}Ca+^{40}Ca$ system is the heaviest one in which their separation is possible, and special attention was given to achieve this aim experimentally.

The Institut de Physique Nucléaire, Orsay, has the facilities to accelerate calcium ions over a very large range of incident energies: (i) Below 170 MeV (lab) with the upgraded M.P. tandem: The intrinsic beam qualities are well within the experimental requirements of such a study. The negative ion source is of the Penning type, and has been described elsewhere.[8] (ii) Above 175 MeV (lab) with the Alice accelerator: Although the qualities of the beam are not as good, the larger intensity permits extension of the tandem results over a large energy range.

With both accelerators, a similar experimental technique (Fig. 1) was used. The apparatus consisted of two solid-state detectors, in which the energies E_1 and E_2 of two kinematically associated particles were measured. Together with a time-difference signal between the detectors, the energy signals were recorded on tape for off-line analysis. Using large-area detectors (50×10 mm^2), positioned 15 cm from the target, the effective solid angle was about 3 msr, whereas the horizontal opening could be kept as small as 0.75°. These values were determined by the use of a specially shaped (elliptic) slit in front of one of the detectors, the second one having a sufficiently large aperture to ensure the maximum coincidence efficiency.

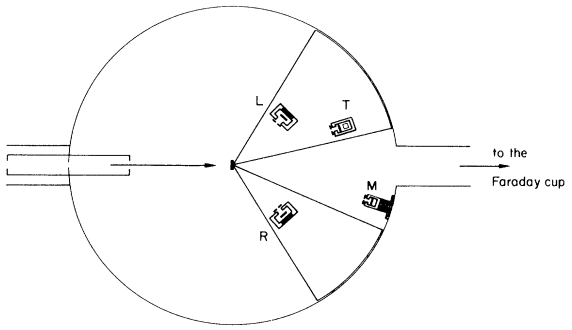

FIG. 1. The scattering chamber and arrangement of the detectors. L and R are the associated detectors, T the ΔE-E telescope, and M a monitor.

Such a method was thought to be more convenient and efficient for the following reasons: (i) The large solid angle allows for the measurement of the small cross sections which are observed around 90° (c.m.). (ii) The kinematical coincidence method is well fitted to a case where the measured energies in each detector are close to each other. (iii) Due to the identity of the incident particles, large oscillations are observed around 90° and the small horizontal opening permits a rather precise determination of the angular distribution. This is crucial in the measurement of the 90° excitation function, where the observation angle has to be known with good accuracy. To achieve this accuracy, the angular distribution was measured over a small angular range at each incident energy. Since the Q values for all reaction channels are negative, the identification of the elastic channel will depend upon the energy resolution of each detector. The resolution of the detectors is found to be 1.1 MeV for the elastic scattering of Ca on Au. This is largely worse than obtained with lighter projectiles, even ^{32}S, and probably due to the larger density of charges created by heavier ions. Two reaction channels might not be separated from the elastic one: (i) the four-particle transfer $^{40}Ca(^{40}Ca, ^{36}Ar_{g.s.})^{44}Ti_{g.s.}$ with a Q value of −1.92 MeV (however, it can be eliminated by analyzing the individual energies in each detector); (ii) the inelastic scattering $^{40}Ca(^{40}Ca, ^{40}Ca)^{40}Ca^*$ to the 3^- state at 3.74 MeV excitation energy in ^{40}Ca.

For the tandem experiment, the target thickness gives the largest contribution to the (E_1+E_2) spectrum width. The overall resolution was found to be about 2.5 MeV. Therefore it can be asserted that, at incident energies smaller than 83 MeV (c.m.) the measured elastic cross sections contain no contribution from any nonelastic channel. At Alice, the overall resolution read on the (E_1+E_2) spectrum is 4 MeV, because of the target thickness and, especially, the beam energy dispersion, and the inelastic transition can give some contamination to the elastic cross sections. At most, the actual elastic cross sections can only be smaller than the values presented. This will be of importance in the discussion on the shape of the excitation functions.

The detectors looked at a 60 μg/cm^2 natural calcium target, evaporated on a 10 μg/cm^2 carbon backing and a gold layer of about 3 μg/cm^2. Due to this target thickness, the uncertainty on the c.m. energy at which the reaction occurs is less than 0.5 MeV though the (E_1+E_2) spectrum resolu-

tion is 2.5 MeV. This 0.5 MeV value was used as the energy step in the measurement of the excitation functions.

At small angles, a ΔE-E telescope was used (where ΔE was obtained from a solid-state detector, the thickness of which was either 8.6 μm or 13.6 μm). This telescope gives the elastic cross section values at small angles ($\theta_{lab} \lesssim 30°$) but it is also convenient to evaluate the population of the different reaction channels at a close-to-grazing angle. The identification was always good enough to separate adjacent elements for $Z \lesssim 25$.

When measuring the elastic scattering over a large range of angles and incident energies, the determination of absolute cross sections is a delicate problem. At very low energies (close to the Coulomb barrier) cross sections oscillate very rapidly, so that accuracy is difficult to obtain. The consistency over the whole set of data was checked, using the 60° and the 70° Mott cross sections at low energy, and the forward cross sections at higher energy where angular distributions do not oscillate. The absolute cross sections over the entire energy range are given within 30%.

III. ANGULAR DISTRIBUTIONS

Five angular distributions are presented in Fig. 2. Two of them are measured with the tandem accelerator ($E_{c.m.} = 64.8$ and 71.8 MeV), two others with the accelerator Alice ($E_{c.m.} = 88$ and 93 MeV). The fifth one is taken from the data of Henning *et al.*[9] at $E_{c.m.} = 55.4$ MeV. At this energy, Coulomb phenomena are still so important that the interference pattern due to the identity of the colliding particles covers the whole angular range. At higher energies, this interference only shows up within a region of about 10° around 90° c.m.

Such a limitation suggests another presentation of the data. As the identity of the particles is found to play only a minor role in the shape of the angular distributions, it appears more meaningful to plot the ratios of the experimental cross sections to the Rutherford cross sections (i.e., to the *non*symmetrized Coulomb cross sections). These ratios are reported in Fig. 3 for six bombarding energies. Except for the lowest incident energy, these curves follow the usual Fresnel pattern.[10]

It has been noticed[11] that the observed large enhancement over the Rutherford cross section value could give information on the influence of the real nuclear potential on the scattering trajectories. Frahn and Venter[12] have shown that the amplitude of this rise increases with the real nuclear phase shift, from the sharp cutoff value:

$$1 + \frac{2}{\pi\sqrt{3}}\left[1 - \left(\frac{3\pi}{4\eta}\right)^{1/2}\right]^{3/2} = 1.23$$

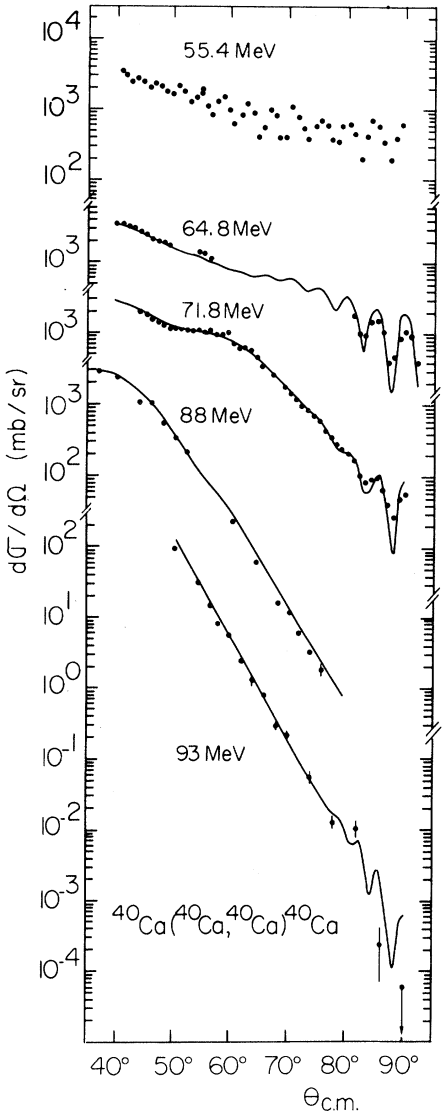

FIG. 2. Angular distributions for the elastic scattering of ^{40}Ca from ^{40}Ca. The solid lines are optical-model predictions. The angular distribution at 55.45 MeV is from Ref. 9.

for $E_{c.m.} = 71.8$ MeV. A smooth cutoff in angular momentum space counteracts the effect of the nuclear attraction. As the data show that this rise is close to 1.23, the "quarter-point recipe"[13] (i.e., the sharp cutoff approximation) can be used to obtain a rough estimate of the distance where nuclear interaction begins to occur. The Fresnel interaction radius and the reaction cross sections as a function of energy are given in Table I, as deduced from the sharp cutoff model from five angular distributions of the Fig. 3. The "quarter-point angular momentum" is obtained from the equation

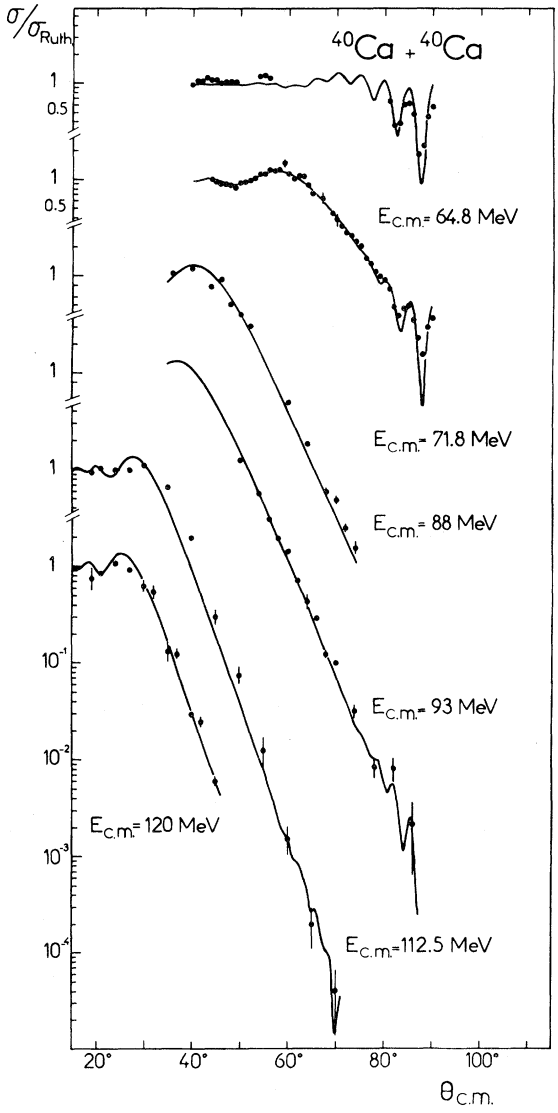

FIG. 3. Ratios of the experimental elastic scattering cross section to the nonsymmetrized Rutherford cross section, as a function of the scattering angle. The solid lines are optical-model predictions.

$$L_{1/4} = \eta \cot(\theta_{1/4}/2) ,$$

where η is the Sommerfeld parameter, and the reaction cross section is given by

$$\sigma_R^{\text{sco}} = \pi \lambda^2 (L_{1/4} + 1)^2 .$$

These values will be compared in Sec. V with those predicted by an optical-model analysis.

The Fresnel interaction radius can be reliably taken as:

$$R = 10.63 \pm 0.13 \text{ fm}; \quad r_0 = 1.55 \pm 02 \text{ fm} .$$

This can be compared with the prediction of

TABLE I. Parameters of the ^{40}Ca + ^{40}Ca elastic scattering. Grazing angular momenta, strong interaction radii, and reaction cross sections as deduced from the sharp cutoff model.

E (MeV)	k (fm^{-1})	η	$L_{1/4}$	R (fm)	σ_R^{sco} (mb)
71.8	8.29	33.25	44.9	10.75	960
88	9.18	30.04	60.9	10.67	1430
93	9.43	29.22	65.6	10.72	1570
112.5	10.4	26.57	77.2	10.42	1780
120	10.7	25.73	84.2	10.61	1980

Huizenga[14] which is

$$R = (2C + 3.2) = 10.47 \text{ fm}; \quad r_0 = 1.53 \text{ fm} ,$$

where C is the half-density matter radius.[15] Since this prediction results from a compilation over a large number of systems, one sees that the ^{40}Ca + ^{40}Ca system does not differ from others from the above viewpoint. Such an interaction distance means that nuclear interactions are at play as soon as one nucleus overlaps the other by about 5% of the central density.

It is more difficult, without referring to an optical-model analysis (as it will be done in Sec. VI), to derive additional information about the absorption in the ^{40}Ca + ^{40}Ca system from the shapes of the angular distribution. Fraunhofer oscillations, if any were to be present, would show up in the backward hemisphere, which in this case cannot be observed because of the symmetry of the entrance channel. On the contrary, the oscillations around 90° in the angular distributions come from that symmetry. No conclusion can be safely drawn from the fact that they are only present over a small angular region, as explained below.

A small reduction of the absorption has two consequences: (i) an increase of the critical angle value and (ii) an enhancement of the forward angle oscillations. Quantitatively, the angular shift is very small, so that the resulting effect is a steeper slope for the angular distribution and thus a narrower angular range for the oscillations. This results in the paradoxical situation where smaller cross sections around 90° are due to a smaller absorption. Thus, the range over which the interference oscillations are present cannot be a very significant test of the importance of the absorption.

IV. EXCITATION FUNCTIONS

In Fig. 4 are presented three excitation functions, measured at 60°, 70°, and 90° (c.m.) from 55 MeV (close to the Coulomb barrier) to 120 MeV (c.m.) incident energy. The parts of these excitation functions corresponding to energies smaller than 83 MeV were obtained at the tandem, and there-

fore, as pointed out in Sec. II, are free of inelastic scattering contaminations. At higher energies, such a contamination cannot be ruled out, due to a poorer resolution, in spite of a careful energy calibration. It results from such a situation that the slopes of these excitation functions, in their high-energy part, could only be steeper. It is clear that these excitation functions, in the reasonably large energy range studied here do not exhibit any gross structure. Had the energy resolution been too bad to observe a structure, a break in the excitation function slopes could have been the energy-average result of some transparency in the interaction potential. These data, up to 120 MeV (c.m.) incident energy, and down to 1 μb/sr cross sections do not indicate such a feature. It can also be noticed that, for the low-energy part of these curves, the 0.5 MeV energy step is thought to be small enough for disclosing any irregularity in the excitation functions. Such irregularities are not found.

To conclude, from the shapes of the excitation functions and angular distributions it appears that, in contradiction to what could have been expected, the elastic scattering behavior of the system studied does not depart from the most commonly used strong-absorption model. This point will be strengthened more quantitatively in the following sections.

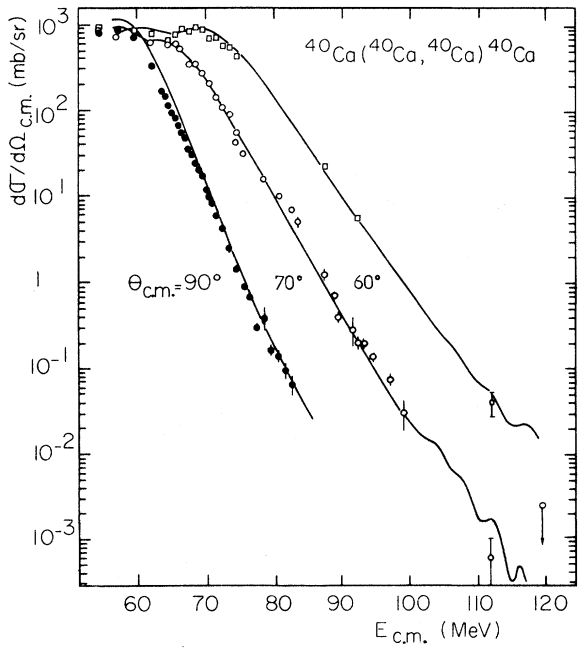

FIG. 4. Excitation functions for the elastic scattering of ^{40}Ca from ^{40}Ca at 60°, 70°, and 90° (c.m.). The solid lines are optical-model predictions.

V. OPTICAL-MODEL ANALYSIS

For such an analysis, a set of data collected over a very large energy range composes a very severe constraint, as first pointed out in the analysis of the $^{16}O+^{16}O$ data.[4] Several searches were carried out, from different initial parameter values. By no means should the present result be taken as unique, but it represents an average result which fits the data fairly well. With a four-parameter optical-model potential

$$V_{opt}(r) = \frac{V+iW}{1+\exp(r-R)/a} + V_{Coul}(r) ,$$

where

$$R = 2r_0(40)^{1/3} ,$$

the following parameter values have been obtained:

$$\begin{aligned} &V = 35 \text{ MeV} , \\ &W = 12.13 \text{ MeV} , \\ &r_0 = r_c = 1.35 \text{ fm} , \\ &a = 0.43 \text{ fm} . \end{aligned} \tag{1}$$

The predictions of this optical-model potential are given by the curves of the Figs. 2–4.

The Igo ambiguity was also observed when checking that all the real potential having the same slope and the same depth at the strong interaction radius (as determined in Sec. III), essentially give the same results. This indicates that only the tail region of the potential is of importance. As can also be deduced from the geometry of the real and imaginary potentials, the W/V ratio is a constant equal to 0.4 which is a smaller value than was formerly proposed.[16] It should be noticed that it has been possible to fit the data without any energy or angular momentum dependence of the imaginary potential. Moreover, the reflection coefficients have the typical behavior (i.e., do not present any "kink") of strong absorption for grazing partial waves. This is illustrated in Fig. 5.

From the computed transmission coefficients, one can compare the predicted total reaction cross section with the one deduced from the strong-absorption model. Such a comparison, as reported in Table II, shows how good the predictions of the latter are; the differences never exceed 5%.

The comparison between the $L_{1/4}$ value as given by the strong-absorption model, and the value L_{opt} for which the reflection coefficient is equal to 0.5, also gives agreement within 5%.

From the classical expression

$$L(L+1) = 2\mu R^2(E-E_B)/\hbar^2 ,$$

where L can be taken as the quantity L_{opt} defined above, the six energies for which angular distri-

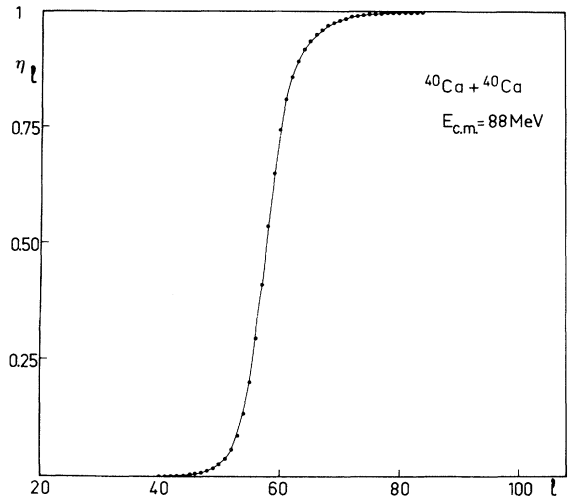

FIG. 5. Plot of the reflection coefficient $\eta(l) = |S(l)|$ as a function of l at 88 MeV (c.m.).

butions were obtained allow for a determination of R and E_B, or rather a check of the consistency of our results. The quantity $L_{\rm opt}(L_{\rm opt}+1)$ is found to be a linear function of E, giving the values

$$r_0 = 1.46 \text{ fm} ,$$

$$E_B = 52.69 \text{ MeV} .$$

In Table II are also reported the values of the quantities Δ and d, defined as follows: Δ represents the width of the transition region on which the reflection coefficients vary from 0 to 1, when fitted by the expression

$$\eta(l) = \{1 + \exp[(L_{\rm opt} - l)/\Delta]\}^{-1} .$$

Classical arguments have been used[17] to show that the energy dependence of Δ could be reproduced by

$$\Delta = kd\left(1 - \frac{\eta}{kR}\right)\Big/\left(1 - \frac{2\eta}{kR}\right)^{1/2} .$$

Here, the value of d, as deduced from this expression, and using the optical-model reflection coefficients, is approximately independent of energy and equal to 0.21 fm. We shall return to this point in Sec. VI.

Several theoretical attempts have been made to estimate the real part of the ^{40}Ca + ^{40}Ca interaction potential. Figure 6 shows the predictions of these potentials. First, a folded potential with an effective interaction

$$V_{\rm eff}(r) = \left(6315\,\frac{e^{-4r}}{4r} - 1961\,\frac{e^{-2.5r}}{2.5r}\right) \text{ MeV}$$

was proposed by Satchler.[18] The imaginary part of the optical potential is taken to have the same geometry as the real one:

$$V_{\rm opt}(r) = (1 + 0.7i)V_{\rm fold}(r) .$$

The satisfactory fit at low energy becomes worse with increasing energy.

TABLE II. Comparison between optical-model predictions and sharp cutoff theory. Δ is the width of the reflection coefficient function in the angular momentum space, and d is the associated thickness at the surface of the nucleus (see text).

E (MeV)	$L_{1/4}$	$L_{\rm opt}$	$\sigma_R^{\rm sco}$ (mb)	$\sigma_R^{\rm OM}$ (mb)	$\Delta_{\rm OM}$	d (fm)
64.8		32.9		669	2.67	0.20
71.8	44.9	42.1	960	939	2.42	0.22
88	60.9	57.7	1430	1390	2.24	0.21
93	65.6	61.7	1570	1495	2.20	0.21
112.5	77.2	75	1780	1808	2.24	0.20
120	84.2	79.4	1980	1900	2.34	0.21

The data are also compared with the predictions of two potentials, calculated from the "sudden approximation": Ngô *et al.*[19] have used the Brueckner energy density formalism, while Stancu and Brink[20] derive the interaction potential from the energy functional of the Skyrme interaction. These two potentials give rather similar results. On the other hand, following a procedure already used by Huizenga,[14] and deduced from the liquid-drop theory, the depth and diffuseness of the potential can be determined from the relations:

$$\left(\frac{dV_N}{dr}\right)_{r=2C} = \frac{V_0}{4a} = 2\gamma C$$

with

$$\gamma = 0.9517 \text{ MeV fm}^{-2} .$$

In that case the nuclear potential is taken to have the right value at the strong interaction radius, but the slope differs from the empirically determined one. For these last three potentials, the imaginary part parameters are those given in Eqs. (1).

In Fig. 7 the radial dependence of all of these potentials has been compared. One sees that the theoretical potentials seem to be systematically more shallow than the empirical one at the strong interaction radius.

From these interaction potentials, it has been shown[21] that one can obtain predictions for fusion cross sections. It is remarkable that all these potentials give about the same predictions. These predictions, reported in Fig. 8 have been obtained from the model of Glas and Mosel.[22] One can see that a determination of the nuclear potential depth at the "critical radius,"[21] here taken as

$$R_{\rm crit} = 2(40)^{1/3} \text{ fm}$$

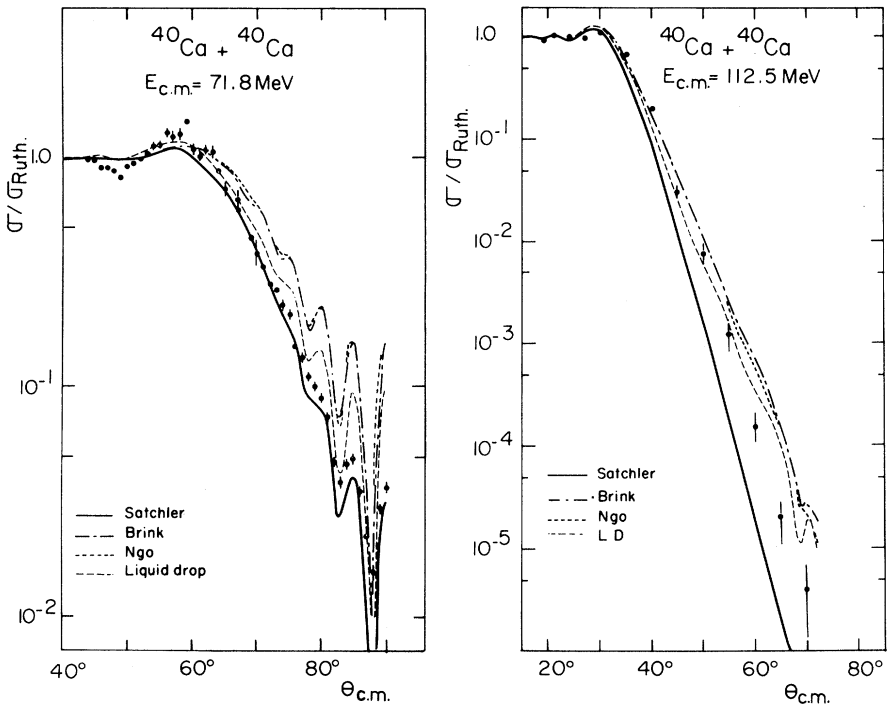

FIG. 6. A comparison between the predictions of several interaction potentials at two incident energies.

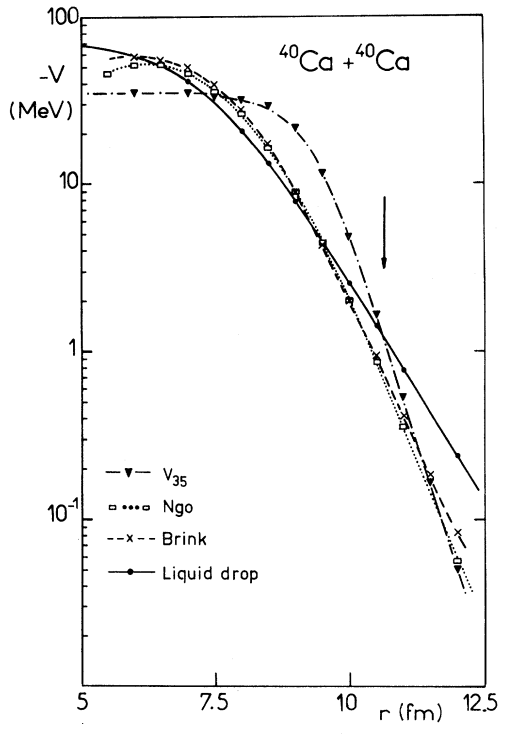

FIG. 7. Comparison of the radial dependence of the real potentials used in optical-model fits. The arrow indicates the strong interaction radius.

could be possible from fusion cross sections, as the predictions from two interaction potentials relevant to the Igo ambiguity but with very different depths are extremely different at high energy.

Thus, a rather good description of the interaction potential for a large separation distance between the ^{40}Ca ions has been obtained. For smaller distances, fusion cross section measurements could help to solve the usual ambiguities.

VI. DISCUSSION OF THE RESULTS

In this section, we wish to compare the ^{40}Ca + ^{40}Ca elastic scattering with that of other heavy-ion systems. It was shown in the preceding sections that the ^{40}Ca + ^{40}Ca elastic scattering does not seem to differ from elastic scattering of neighboring systems. However, one of the motivations of this study was the similarity between the structure of the ^{16}O and ^{40}Ca nuclei. In a comparison between the experimental data, it can immediately be seen that the ^{40}Ca + ^{40}Ca angular distributions and excitation functions exhibit the Fresnel pattern, while the ^{16}O + ^{16}O scattering shows a behavior close to Fraunhofer diffraction.

For nuclei of mass close to 16, the excitation functions are characterized by the presence of comparable gross structure. For ^{28}Si + ^{28}Si or ^{40}Ca + ^{40}Ca, the elastic scattering excitation func-

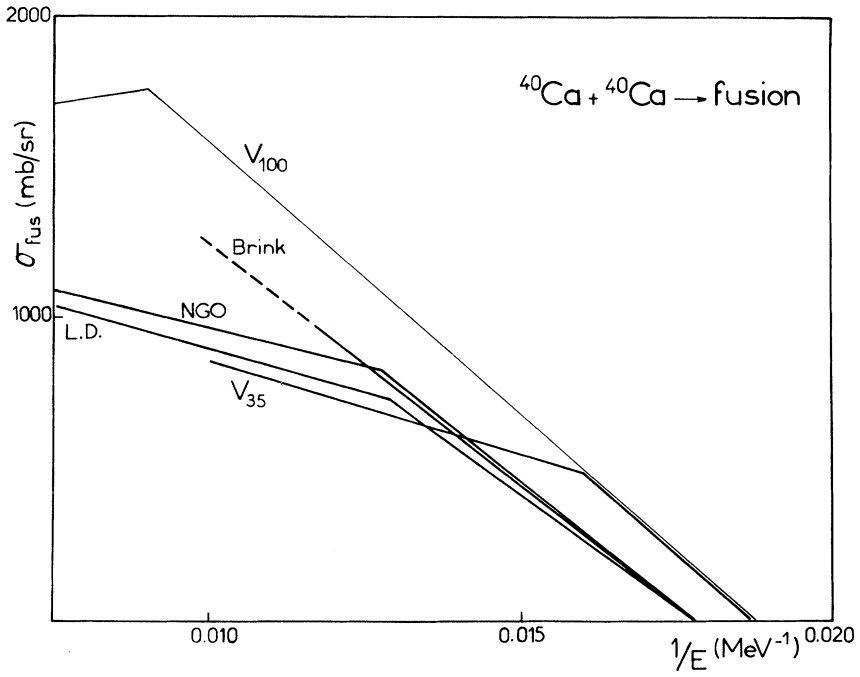

FIG. 8. Glas and Mosel predictions of the fusion cross sections as a function of energy, for several interaction potentials. V_{35} is the potential used in the optical-model analysis. V_{100} and V_{35} satisfy the same Igo criterion $V \exp(R/a) = \text{const}$.

tions are monotonically decreasing. Thus, it appears that maybe the consequence of the larger mass and charge has to be analyzed when comparing data.

At this point, it may be worthwhile to recall the interpretation of the structure observed in excitation functions for masses close to 16. This structure is considered to be evidence for some transparency of the interaction potential for the grazing partial waves. At a given energy, only a single partial wave gives the leading contribution to the scattering amplitude, the others being either absorbed or reflected, and therefore the observed structure appears to be due to the succession of the leading partial waves when the incident energy is increased.[23] As shown by Siemssen,[24] the degree of transparency of the effective potential can be read on the distribution of the reflection coefficients as a function of the angular momentum. In a strong-absorption case, this distribution goes smoothly from 0 to 1, and a rather large number of partial waves give a limited contribution to the elastic scattering amplitude. On the contrary, in the $^{16}O + ^{16}O$ and other weak-absorption cases, this transition occurs within a narrow range of angular momenta.

The structures have been reproduced by optical-model calculations either by reducing[23] the range of the imaginary well as compared to the real one, or through an explicit l dependence of the imaginary well depth.[5] The introduction of this l cutoff in the absorption mechanism leads to enumeration of the exit channels which are able to carry out the entrance angular momentum. Transparency is then observed when such channels do not exist at the incident energy considered. Comparing the $^{16}O + ^{16}O$ and $^{18}O + ^{18}O$ data, Shaw, Vandenbosch, and Mehta[6] proposed that only the direct channels are to be taken into account in such an enumeration. Thus, a structure can be expected when no direct channel is able to carry away the incident angular momentum. This should be the case for $^{40}Ca + ^{40}Ca$, on the basis of Q values for direct transfers.

However, in spite of its large experimental support, such an analysis presents some shortcomings. For instance, as one is interested in the role of the energy in the observation of a gross structure, one could predict from the above criterion that the structure observed in $^{16}O + ^{16}O$ elastic scattering should disappear with increasing energy for $E_{c.m.} \gtrsim 25$ MeV, since several direct channels can then carry away the entrance angular momentum. This is at variance with experimental data,[25] at least if the structure observed in the excitation function is considered to be relevant to the same physical phenomenon. On the other hand, such a structure was only observed for nuclei of

mass close to 16, and in the $^{18}O+^{18}O$ case used as an example of strong absorption by Shaw *et al.*,[6] some bumps still show up in the excitation function. This is not even the case for $^{40}Ca+^{40}Ca$. Finally, as mentioned in Sec. II, the importance of transfer reactions has been estimated. Their cross sections are found to be extremely low up to $E_{c.m.}=75$ MeV, and then slowly increasing with energy. Thus, it has been verified experimentally that the conditions necessary for a structure are fulfilled.

A major difference between the ^{16}O and the ^{40}Ca systems is the much stronger Coulomb repulsion in the latter and it will be attempted to show how this can explain the gradual disappearance of the gross structure going from ^{16}O to ^{40}Ca.

To obtain further insight into this problem, it is convenient to split the scattering amplitude into two terms, using the asymptotic expansion of the Legendre polynomials

$$P_l(\cos\theta) \simeq \left(\frac{2}{\pi(l+\frac{1}{2})\sin\theta}\right)^{1/2} \cos[(l+\tfrac{1}{2})\theta - \tfrac{1}{4}\pi]$$

valid for $l \gg 1$ and $\theta \gg l^{-1}$.

Assuming a smooth variation of both the reflection coefficients $\eta(l)$ and the nuclear phase shifts $\delta^N(l)$ over a range Δ of l values around a central value L, we can use the semiclassical approximation of the scattering amplitude:

$$f(\theta) = -\frac{i}{k}\left(\frac{1}{2\pi\sin\theta}\right)^{1/2} \int_0^\infty d\lambda\, \lambda^{1/2}\eta(\lambda) e^{2i\delta(\lambda)}\left[e^{i(\lambda\theta-\pi/4)} + e^{-i(\lambda\theta-\pi/4)}\right]$$
$$= f_+(\theta) + f_-(\theta)$$

with $\lambda = l + 0.5$.

For large angles (i.e., beyond a "critical" value θ_c) and under the condition that the deflection function has no rainbow, Frahn[26] obtains the following closed expression:

$$f(\theta) = f_-(\theta) + f_+(\theta) = \frac{1}{k}\left(\frac{1}{2\pi\sin\theta}\right)^{1/2} e^{2i\delta(\Lambda)}\left\{e^{-i(\Lambda\theta-\pi/4)} A(\theta-\theta_c) F[\Delta(\theta-\theta_c)] + e^{i(\Lambda\theta-\pi/4)} F[\Delta(\theta+\theta_c)]/(\theta+\theta_c)\right\} , \quad (2)$$

where $\Lambda = L + 0.5$.

To examine the outcome of such a separation, we have to use an analytic approximation for the scattering S matrix. Following Frahn, we use the McIntyre[27] parametrization:

$$S(\lambda) = \eta(\lambda)\, e^{2i\delta(\lambda)} ,$$

$$\eta(\lambda) = \left[1 + \exp\left(\frac{\Lambda-\lambda}{\Delta}\right)\right]^{-1} ,$$

$$\delta(\lambda) = \sigma(\lambda) + \delta_0\left[1 + \exp\left(\frac{\lambda-\Lambda'}{\Delta'}\right)\right]^{-1} .$$

It is understood that this parametrization does not fit exactly every feature of the optical-model S matrix, especially as far as the real nuclear phase shifts are concerned. However, it is considered as sufficiently reliable to reproduce the main characteristics of the cross section. Then

$$F[\Delta x] \equiv \int_{-\infty}^{+\infty} d\lambda \frac{d}{d\lambda}\eta(\lambda) e^{-i(\lambda-\Lambda)x} = \frac{\pi\Delta x}{\sinh(\pi\Delta x)} .$$

It should be noted that the expression of $f_+(\theta)$ does not depend upon the condition of no rainbow in the deflection function, but only on the linear expansion of the phase about $\lambda = \Lambda$. Thus, whatever the S matrix is, $f_+(\theta)$ can always be calculated, and substracted from the full $f(\theta)$ obtained by the partial wave summation to obtain $f_-(\theta)$.

To further simplify Eq. (2), we assume that

$$A(\theta-\theta_c) \cong -1/(\theta-\theta_c) . \quad (3)$$

It can be shown that for "ordinary cases," this approximation is of no consequence.

As we are interested in the energy dependence of $f(\theta)$, one has to assume some variation of the parameters with energy. Frahn has used the following:

$$\Lambda = kR(1-2\eta/kR)^{1/2} ,$$
$$\Delta = kd(1-\eta/kR)/(1-2\eta/kR)^{1/2} , \quad (4)$$
$$\delta_0 = \alpha/k$$

with

$$R = r_0(A^{1/3}{}_1 + A^{1/3}{}_2)$$

and Λ' and Δ' introduce two more parameters r_0' and d' through similar relations.

Within this framework, we will examine the elastic scattering of $^{16}O+^{16}O$ and $^{40}Ca+^{40}Ca$.

A. $^{40}Ca+^{40}Ca$

Frahn and Rehm[28] have been able to fit the $^{40}Ca+^{40}Ca$ data presented in this paper, with the following parameter set: $r_0 = 1.584$ fm, $r_0' = 1.438$ fm, $\alpha = 154^\circ\,\text{fm}^{-1}$, $d = 0.286$ fm, $d' = 0.58$ fm. The quantities r_0 and d can be compared with those de-

termined in the optical-model analysis (Sec. V). It can be observed that d is close to one-half of the optical-model diffuseness a [28] and that the phase does not give rise to a rainbow.

With these values, both components $|f_+(\theta)|$ and $|f_-(\theta)|$ are monotonically varying with energy. Over the whole energy range studied, $|f_+|$ is several orders of magnitude less than $|f_-(\theta)|$, and does not give any significant contribution to the cross section. Obviously no interference pattern can be observed. This conclusion is found to be unaffected by reasonable variations of the parameters.

B. $^{16}O+^{16}O$

For this system, it has not been possible to obtain an accurate fit of the excitation functions. This is attributed to the limitations introduced by the McIntyre parametrization. The structure phenomenon can be reproduced, particularly its periodicity and the location of the maxima, with the following parameter set: $r_0 = 1.45$ fm, $r_0' = 1.438$ fm, $\alpha = 100°\ \text{fm}^{-1}$, $d = 0.06$ fm, $d' = 0.58$ fm. However, the peak-to-valley ratio is poorly accounted for. As in $^{40}Ca+^{40}Ca$, it is found that $|f_+|$ and $|f_-|$ vary monotonically with angle and with energy. The main difference between the two systems is that in $^{16}O+^{16}O$, $|f_+|$, although somewhat smaller than $|f_-|$, is sufficiently large to give rise to interference effects. The relative phase between both interfering amplitudes is close to $e^{i(2\Lambda\theta+\pi)}$. Thus one finds that the maxima of the 90° excitation function correspond to odd integer values of Λ. The 60° excitation function should present maxima with a period 1.5 times larger than at 90°. This is precisely observed in Fig. 9, where the predictions of the optical-model potential proposed by Gobbi *et al.*[23] for the $^{16}O+^{16}O$ elastic scattering excitation functions at 60° and 90°, and the Λ values deduced from the reflection coefficients are reported [as will be said later, the reflection coefficient function $\eta(l)$ is far from following the Fermi function considered above, but the central value should not be doubtful]. The fact that this behavior is satisfactorily reproduced is considered a good test of the reliability of the approximations introduced above.

C. Influence of the mass on the occurrence of a gross structure

The obvious conclusion of the study of these two systems is that the gross structure seen in the elastic scattering excitation function for light nuclei finds its origin in the interference between $f_+(\theta)$ and $f_-(\theta)$. It is therefore crucial to study the ratio

$$R = \left|\frac{f_+}{f_-}\right|$$

of these two quantities, as the value of this ratio will determine the strength of the interference effect. Within the McIntyre parametrization this ratio is given by

$$R \simeq \frac{\sinh[\pi\Delta(\theta-\theta_c)]}{\sinh[\pi\Delta(\theta+\theta_c)]} \simeq e^{-2\pi\Delta\theta_c} \ . \tag{5}$$

At the same reduced energy

$$h = \frac{E}{B_C} \ ,$$

where B_C is the Coulomb barrier and θ_c is the same. Thus one finds that R exponentially depends

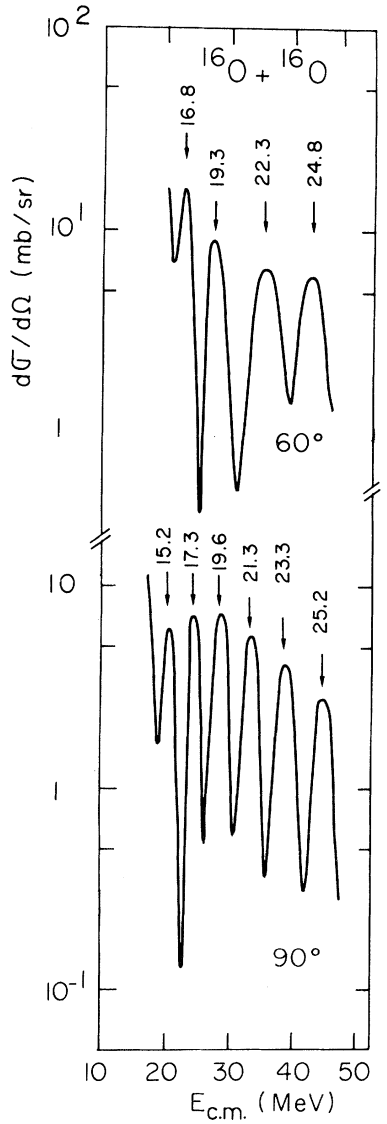

FIG. 9. $^{16}O+^{16}O$ excitation functions at 60° and 90° as predicted by the Gobbi potential. The numbers indicated at the maxima of the cross section denote the values of Λ for the corresponding energies.

on Δ. This quantity as given by Eqs. (4) can be written for $A = 2Z$ nuclei:

$$\Delta = 3.3\times10^{-2}\frac{d(2h-1)}{[r_0(h-1)]^{1/2}}A^{4/3}\,. \tag{6}$$

In Fig. 10 the ratio R is plotted as a function of h, for the three systems ^{16}O + ^{16}O, ^{28}Si + ^{28}Si, and ^{40}Ca + ^{40}Ca. The curves have been obtained using the same set of parameters, to point out the mass dependence. The values of d and r_0 which have been used are mean values of those fitting the ^{16}O + ^{16}O and the ^{40}Ca + ^{40}Ca excitation functions.

Equations (5) and (6) show the exponential dependence of R on the mass (or charge) of the colliding nuclei. This explains the differences in behavior observed in Fig. 10. Within the framework of this parametrization, it is immediately clear that for light nuclei, a large interference can be expected, so that structure in the cross sections is easily observed, even at low energies, whereas for heavier mass systems a similar phenomenon can only be obtained at very high energy. The above discussion was based on the dependence of Δ on A; however, Eq. (6) shows that Δ varies linearly with d, which is closely related to the absorptive part of the interaction. This explains the differences between ^{16}O + ^{16}O and the neighboring systems.[6]

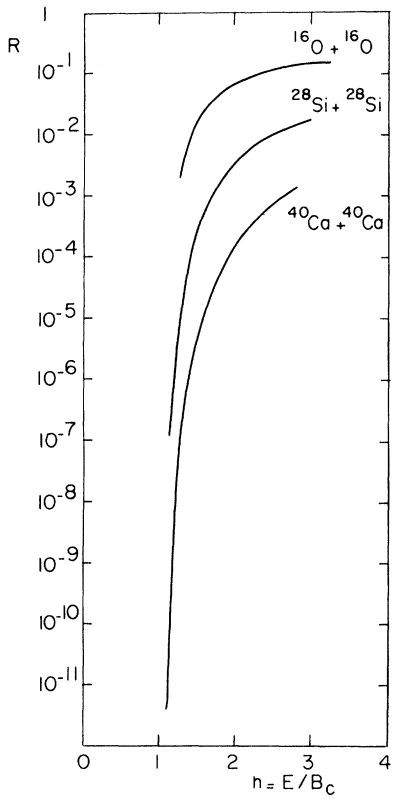

FIG. 10. Plot of the ratio $R = |f_+/f_-|$ (see text) which determines the magnitude of a structure in the excitation functions for three systems of identical nuclei. The parameters used are the following: $r_0 = 1.584$ fm, $d = 0.2$ fm, $r_0' = 1.438$ fm, $d' = 0.58$ fm, $\alpha = 60°$ fm^{-1}.

All these observations seem to be based upon the McIntyre parametrization. However, as shown in Eq. (5), the quantity R only depends on the Fourier transform of the "absorptive shape functions," and also on the value of θ_c. The latter is connected to the shape of the deflection function, and the former to the slope of the function $\eta(l)$. This point has been particularly analyzed by Siemssen *et al.* in their study[29] of the ^{16}O + ^{18}O elastic scattering, as they point out the presence of "kinks" in the function $\eta(l)$, which should affect the Fourier transform $F(\Delta x)$. Another presentation of the same analysis is the introduction[30] of Regge poles in the S matrix to produce these kinks. A quantitative analysis of this situation will be the subject of a separate study.[31] Whatever the importance of these two points for the elastic scattering of light nuclei is, it does not seem that their effects should modify the qualitative conclusions which result from the interpretation in terms of interference.

The purpose of this discussion is to point out that, beyond the specific behavior of each heavy-ion (the signature of which is the possibility of rainbows, kinks ...), there exists, as one goes from ^{12}C to ^{16}O to ^{28}Si and ^{40}Ca, a very strong effect which damps the interference between the two terms of the amplitude. Frahn has shown[10] that this effect, essentially due to the Coulomb repulsion, is similar to the one of a diverging lens.

Thus, even though a parametrization is difficult to find in the ^{16}O + ^{16}O case, which means that this nucleus has a very specific interest, it remains that the main conclusions of the Frahn model can be used to predict the occurrence of a structure. For instance, it is readily understood how oscillations have been observed in the ^{13}C + ^{40}Ca elastic scattering angular distributions by the Brookhaven group,[32] and how the peak-to-valley ratio decreases strongly in the elastic scattering excitation functions when one goes from ^{16}O + ^{16}O to ^{16}O + ^{28}Si.[33]

VII. CONCLUSION

The elastic scattering of ^{40}Ca by ^{40}Ca has been studied over a large range of incident energies, and six angular distributions have been presented. A sharp cutoff model analysis has given an interaction distance of $r_0 = 1.55$ fm (corresponding to overlap for densities equal to 5% of the central density). The optical-model potential which was found to fit the data has a W/V ratio equal to 0.4, considerably smaller than had been found former-

ly. This potential has neither energy nor angular momentum dependence, and the geometries for both wells are identical.

From these results, it appears that the magic of ^{40}Ca does not seem to play an important role in the elastic scattering. No evident transparency shows up, and three excitation functions, measured from the Coulomb barrier to twice this value with a sufficiently small energy step, are monotonically decreasing over this range of incident energies.

Thus, the analogy with the $^{16}O+^{16}O$ system which was looked for is not found. However, it has been possible to show that the larger mass and charge in the ^{40}Ca case would make the observation of such a structure unlikely, even if the studied system had presented some transparency for the grazing partial waves. A specific behavior of the ^{40}Ca nucleus would have to be searched for with a lighter projectile or in a comparison with other systems, as for example $^{40}Ar+^{40}Ca$ or $^{40}Ca+^{44}Ca$.

ACKNOWLEDGMENTS

We would like to express our gratitude to Dr. C. Marty for many enlightening discussions. We thank Professor W. E. Frahn for the interest he has shown for this experiment, and for kindly sending us his results prior to publication. We are also grateful to Dr. G. R. Satchler for allowing us to present the predictions of the folded potential. We would like to thank P. Martin and P. De Saintignon for the part they took in this experiment. We are greatly indebted to M. Dumail and her group for the qualities of the negative Ca ion source. We thank the operating crews of the tandem and Alice accelerators for their assistance, and L. Stab and his group for providing us with the large area detectors.

*Present address: D PhN/BE, CEN Saclay, BP No. 2, 91190 Gif/Yvette, France.

[1]J. R. Birkelund, J. R. Huizenga, H. Freisleben, K. L. Wolf, J. P. Unik, and V. E. Viola Jr., Phys. Rev. C 13, 133 (1976); R. Vandenbosch, M. P. Webb, T. D. Thomas, S. W. Yates, and A. M. Friedman, *ibid.* 13, 1893 (1976).

[2]P. Bonche, S. Koonin, and J. W. Negele, Phys. Rev. C 13, 1226 (1976); S. Koonin, Phys. Lett. 61B, 227 (1976); R. Y. Cusson, R. K. Smith, and J. A. Maruhn, Phys. Rev. Lett. 36, 1166 (1976).

[3]P. Colombani, N. Frascaria, J. C. Jacmart, M. Riou, C. Stéphan, H. Doubre, N. Poffé, and J. C. Roynette, Phys. Lett. 55B, 45 (1975).

[4]J. V. Maher, M. W. Sachs, R. H. Siemssen, A. Weidinger, and D. A. Bromley, Phys. Rev. 188, 1665 (1969).

[5]R. A. Chatwin, J. S. Eck, D. Robson, and A. Richter, Phys. Rev. C 1, 795 (1970).

[6]R. W. Shaw, R. Vandenbosch, and M. K. Mehta, Phys. Rev. Lett. 25, 457 (1970).

[7]A. J. R. Ferguson, in Proceedings of the Symposium on heavy-ion scattering [Argonne National Laboratory Report No. ANL 7837, 1971 (unpublished)], p. 187.

[8]M. Dumail and J. P. Mouffron, Nucl. Instrum. Methods 127, 157 (1975).

[9]W. Henning, P. Müller, M. Richter, H. P. Rother, K. E. Rehm, H. Schaller, and H. Spieler, University of Munich Annual Report, 1972 (unpublished), p. 24.

[10]W. E. Frahn, Ann. Phys. (N.Y.) 72, 524 (1972).

[11]N. Rowley, Nucl. Phys. A239, 134 (1975).

[12]W. E. Frahn and R. H. Venter, Ann. Phys. (N.Y.) 24, 243 (1963).

[13]J. S. Blair, Phys. Rev. 95, 1218 (1954).

[14]J. R. Huizenga, in Proceedings of the Symposium on macroscopic features of heavy-ion collisions [Argonne National Laboratory Report No. ANL/Phy. 76-2, 1976 (unpublished)], p. 1.

[15]W. D. Myers, Nucl. Phys. A204, 465 (1969).

[16]H. Doubre, J. C. Roynette, J. C. Jacmart, N. Poffé, M. Riou, E. Plagnol, and P. De Saintignon, Phys. Rev. Lett. 35, 508 (1975).

[17]J. S. Blair, in *Lectures in Theoretical Physics*, edited by P. D. Kunz and W. E. Brittin (Univ. of Colorado Press, Boulder, Colorado, 1966), Vol. VIII C, p. 343.

[18]G. R. Satchler (private communication).

[19]C. Ngô, B. Tamain, J. Galin, M. Beiner, and R. J. Lombard, Nucl. Phys. A240, 353 (1975).

[20]F. Stancu and D. M. Brink, Nucl. Phys. A270, 236 (1976).

[21]J. Galin, D. Guerreau, M. Lefort, and X. Tarrago, Phys. Rev. C 9, 1018 (1974).

[22]D. Glas and U. Mosel, Nucl. Phys. A237, 429 (1975).

[23]A. Gobbi, R. Wieland, L. Chua, D. Shapira, and D. A. Bromley, Phys. Rev. C 7, 30 (1973).

[24]R. H. Siemssen, in *Nuclear Spectroscopy and Reactions*, edited by J. Cerny (Academic, New York, 1973), Part B, p. 233.

[25]M. L. Halbert, C. B. Fulmer, S. Raman, M. J. Saltmarsh, A. H. Snell, and P. H. Stelson, Phys. Lett. 51B, 341 (1974).

[26]W. E. Frahn, in *Heavy Ion, High Spin States and Nuclear Structure* (IAEA, Vienna, 1975), p. 157.

[27]J. A. McIntyre, K. H. Wang, and L. C. Becker, Phys. Rev. 117, 1337 (1960).

[28]W. E. Frahn and K. E. Rehm (unpublished) and private communication.

[29]R. H. Siemssen, H. T. Fortune, A. Richter, and J. W. Tippie, Phys. Rev. C 5, 1839 (1972).

[30]K. W. McVoy, Phys. Rev. C 3, 1104 (1971).

[31]E. Plagnol, H. Doubre, and C. Marty (unpublished).

[32]P. D. Bond, J. D. Garrett, O. Hansen, S. Kahana, M. J. Levine, and A. Z. Schwarzschild, Phys. Lett. B47, 231 (1973).

[33]R. H. Siemssen, in Proceedings of the Symposium on heavy-ion scattering [Argonne National Laboratory, Report No. ANL 7837, 1971 (unpublished)], p. 145.